FINAL PROJECT REPORT

Project Title: Identify apple genes associated with apple replant disease resistance

PI: Yanmin Zhu
Organization: TFRL-ARS-USDA
Telephone: (509) 664-2280
Email: yanmin.zhu@ars.usda.gov
Address: 1104 N. Western Ave
Wenatchee, WA 98801

Co-PI: Mark Mazzola
Organization: TFRL-ARS-USDA
Telephone (509) 664-2280
Email: mark.mazzola@ars.usda.gov
Address: 1104 N. Western Ave
Wenatchee, WA 98801

Cooperators: Gennaro Fazio, apple rootstock breeder, USDA ARS

Agency Name: USDA ARS Tree Fruit Research Lab
Amount awarded: **Year 1: $**54,000 **Year 2: $**55,000

Budget history:

Contract Administrator: Charles Myers, Extramural Agreements Specialist		
Email:cwmyers@pw.ars.usda.gov		
Item	**Year 1**	**Year 2**
Salaries *	38,790	38,790
Benefits	13,577	13,577
Wages		
Benefits		
Equipment		
Supplies	1,633	1,733
Travel		
Miscellaneous		
Total	54,000	55,000

*The **salaries and benefits** are budgeted for a GS-7 technician dedicated to this project.

OBJECTIVES

1. Select candidate apple genes based on the results of two previous genomic studies.
2. Screen these genes based on their expression behaviors between resistant and susceptible apple rootstocks.
3. Validate gene-trait associations within an expanded germplasm collection of a rootstock breeding population.

SIGNIFICANT FINDINGS

1. A working phenotyping protocols was established to characterize the biological basis between field observed ARD tolerant G.935 and susceptible B.9 apple rootstocks at the biological and microscopic levels.

2. A total of 43 apple genes were selected to test their expression behavior during *P. ultimum* infection among different rootstock genotypes.

3. Several apple genes related to plant secondary metabolism showed differential patterns of expression among rootstock cultivars with contrasting resistance responses.

4. Preliminary phenotyping data indicated a wider spectrum of resistance responses to infection by *P. ultimum* among O3 x R5 progeny.

RESULTS AND DISCUSSION

1. Phenotypic characterization of apple root resistance response using a streamlined protocol

Establishing the phenotyping protocol. Reliable phenotypes are essential for any molecular genetics study. Considerable effort resulted in the establishment of a streamlined protocol for characterizing the detailed apple root responses to pathogen infection. In the current study, *P. ultimum* was used as a primary ARD model pathogen, although a preliminary experiment was also carried out using other ARD pathogens. Taking the tolerant G.935 and the susceptible B.9 rootstock cultivars as examples, the resistance responses in apple root tissues were carefully examined at both biological and microscopic levels. In brief, the synchronized tissue culture processes were used to propagate both B.9 and G.935 plants with defined genetic background and equivalent ages for *P. ultimum* inoculation assay. As shown in **Figure 1**, similar root masses and root generating patterns were observed between B.9 and G.935 by this tissue culture procedure. A one-week "in-soil" acclimation period to condition the root tissues in the soil environment is necessary to ensure reliable resistance phenotypes for all these tissue-culture generated plants. Plants of both genotypes were inoculated with the same preparation of pathogen inoculum and under identical greenhouse management. For susceptible B.9, the wilt symptoms on the above-ground tissue were observable at 3 dpi. The necrosis patterns in root tissue inoculated with *P. ultimum* were observed at 1, 2, 3, 7 and 14 days post inoculation (dpi); plant survival rate, root biomass, shoot biomass and maximum root length for surviving plants were scored at 30 dpi. The same established procedure was used to assay the individual accessions within the O3 x R5 population.

Genotype-specific survival rate and biomass in response to *P. ultimum* infection. As shown in **Figure 2**, all inoculated G.935 plants except one survived; in contrast, only about 25% of B.9 plants were still alive at 14 dpi. Based on the repeats of inoculation assay, 97% of inoculated G.935 survived compared to 25 % for B.9 plants (**Figure 3**). Noticeably, a few inoculated G.935 plants (less than 5% of total tested) demonstrated light wilt symptoms around 7 dpi, but symptoms disappeared at 14 dpi. Differential responses in terms of root biomass fresh weight, maximum root length and shoot biomass fresh weight were observed among surviving G.935 and B.9 plants at 30 dpi (**Table 1**). Between mock inoculated and *P. ultimum* inoculated

G.935 plants, no statistically significant differences were observed in root biomass and root maximum length; although a 30% reduction in shoot biomass was observed. The observed reduction in shoot biomass suggested that the intrinsic functionality of the root system was partially compromised, even though there was no statistic difference in overall plant survival rate, root biomass and maximum root length. In contrast, shoot biomass for the surviving B.9 plants decreased 68% at 30 dpi compared to the mock inoculated B.9 plants. Similarly, total root biomass and maximum root length for surviving B.9 plants demonstrated a 70% and 40% reduction compared to those of mock inoculated B.9 plants. These observations represent the first evidence of a genotype-specific response among apple rootstocks to challenge by a representative ARD pathogen under controlled conditions.

Figure 1. Images of root system in culture medium and plants for in-soil acclimation. Left panels: Top images: G.935; bottom images: B.9. Images showed the comparable root system between B.9 and G.935 after three-week root induction in tissue culture medium immediately before in-soil acclimation. Right panels: images of plants after one-week in-soil acclimation and before *P. ultimum* inoculation. Top images: G.935; bottom images: B.9.

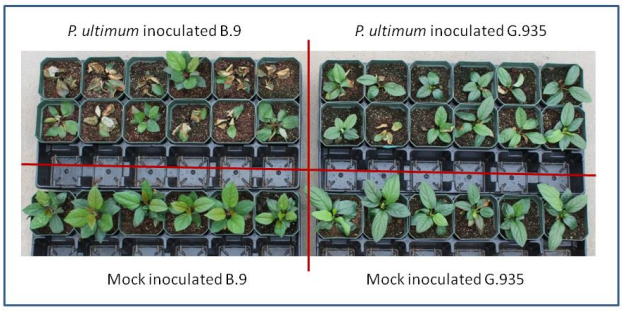

Figure 2. Images of a typical inoculation assay at 14 dpi. At the lower sections are the images of mock-inoculated plants for both B.9 (left) and G.935 (right); the upper panels are the images for *P. ultimum* inoculated plants, similarly B.9 plant on the left and G.935 on the right. The control plants are larger size of compared to *P. ultimum* inoculated and survived plants.

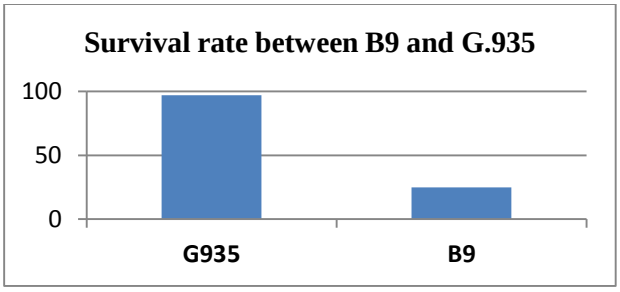

Figure 3. Survival of *Pythium ultimum* inoculated plants a percentage of the mock-inoculated control plants (y-axis is percent). The values were based on at least 155 plants for each cultivar in two independent infection assays.

Table 1. Root biomass, shoot biomass and maximum root length of mock inoculated and *Pythium ultimum* inoculated G.935 and B.9 plants.

	G.935		B.9	
	Mock inoculation	*P. ultimum* inoculation	Mock inoculation	*P. ultimum* inoculation
Root biomass (Fresh weight in g)	1.23 ± 0.31[a]	1.21 ± 0.42[a]	1.12 ± 0.43[a]	0.34 ± 0.10[b]
Maximum Root length (cm)	12.5 ± 3.90[a]	12.3 ± 3.32[a]	11.97 ± 4.91[a]	7.44 ± 4.5[b]
Shoot biomass (Fresh weight in g)	1.40 ± 0.33[a]	0.98 ± 0.26[b]	1.38 ± 0.51[a]	0.43 ± 0.33[b]

The means and standard deviations were based on the values of at least 155 survived plants for mock inoculated G.935, mock inoculated B.9 and *P. ultimum* inoculated G.935 in two independent inoculation assays. At least 40 survived B.9 plants were included from *P. ultimum* inoculated treatment. Means in a row designated with the same letter do not differ according to *t* test, with P <0.05.

Differential root necrosis patterns between B.9 and G.935. No identifiable symptoms were observed on roots of G.935 or B.9 at one day after *P. ultimum* inoculation. At 2 dpi, the majority of G.935 root system remained healthy, showing characteristic white-color root tissues, except localized discolored areas along the root (left panels in **Figure 4A**, arrows). In contrast, symptoms were easily identified on inoculated roots of B.9 (right panels in **Figure 4A**, arrows). The typical symptoms were brown-colored root sections with collapsed or compressed tissues. Uninfected root sections were visible, though rare among B.9 roots. Minor wilt symptoms were observed on leaves for some inoculated B.9 plants. At 7 dpi, larger section of necrosis was easy to spot (left panel in **Figure 4B)**, yet most part of the root system were still healthy as indicated by the typical white color of G.935 roots. Noticeably, the relatively well defined zones which separate the healthy and infected root sections were easily identifiable (left panels in **Figure 4B**) as indicated by arrow. On the other hand, almost the entire B.9 root system was necrotic and brown colored at 7 dpi (right panels in **Figure 4B**). Upon closer examination, hyphae of *P. ultimum* were emerging profusely from infected root tissue (arrow on the images at the right bottom).

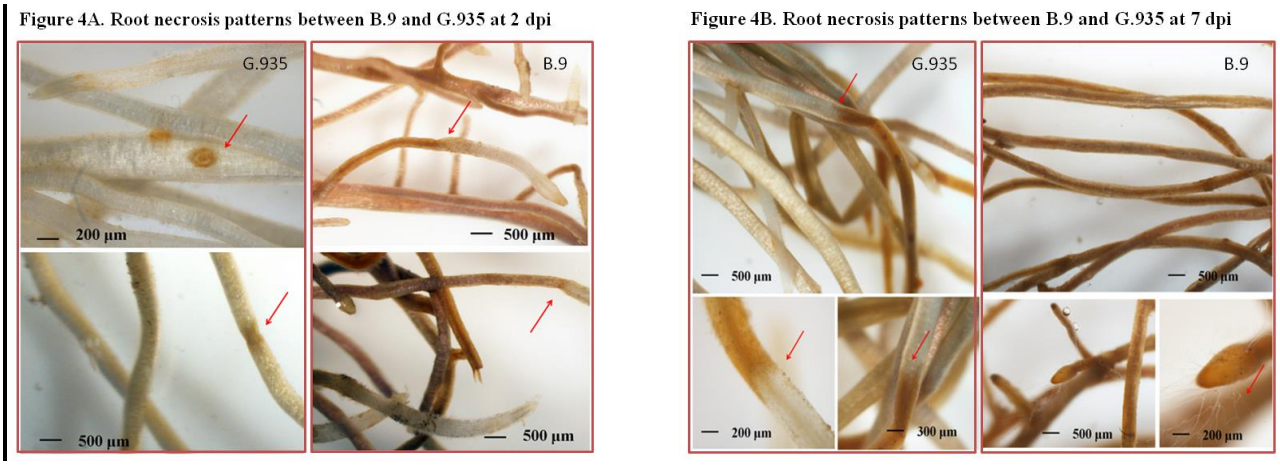

Figure 4. Microscopic images of infected roots for both tolerant G.935 and susceptible B.9. A. the box at left side, root images for both G.935 and B.9 at 2 dpi; B. The box at right, root images for both G.935 and B.9 at 7 dpi. Images show typical symptoms observed using three plants for each of two independent infection assays.

In summary, differential dynamics in necrosis development were observed along the roots of G.935 and B.9. The roots of G.935 exhibited an effective deterrence to pathogen progression, as indicated by limited or localized root necrosis at 2 dpi and a defined separation zone between healthy and necrotic tissue at 7

dpi. In contrast, the B.9 root demonstrated an inability to limit pathogen progression, resulting in rapid development of necrosis and discoloration across the entire root system at 7 dpi.

Field evaluation has indicated that apple rootstock cultivar G.935 is more tolerant to ARD compared to B.9, but the underlying biological bases and molecular mechanisms behind variation in field performance are unknown. Results from this study indicate that the disparity between the G.935 and B.9 resistance responses, in terms of plant survival rate, shoot and root biomass and patterns of root tissue necrosis, is the result of effective functional resistance mechanisms that exist in the roots of tolerant G.935, but not in B.9.

2. Selection of the apple candidate genes

Forty three (43) apple candidate genes, as shown in **Table 2**, were selected for initial analysis of their expression patterns during the infection process among core rootstock varieties with different responses to ARD. The selection of these genes was based on a previous transcriptome analysis, which identified the global gene expression network in apple roots in response to *P. ultimum* infection (1-96 hours after inoculation). Several groups (or families) of genes with annotated function in or regulation of plant secondary metabolism were the primary targets during the candidate gene selection. Many of these genes have multiple closely related members in the apple genome, and therefore initial screenings were performed.

Table 2. Selected apple genes for expression pattern analysis among apple rootstock germplasm

Gene name	Annotated functions	Apple gene identifiers
Chitin Elicitor Receptor Kinase	Pathogen detection	MDP0000136494
Aminocyclopropane-1-carboxylate synthase (ACS)	Ethylene biosynthesis	MDP0000435100, MDP0000130748, MDP0000262827
Allene oxide synthase (AOS)	JA biosynthesis	MDP0000132456, MDP0000195885, MDP0000230092
lipoxygenase (LOX)	JA biosynthesis	MDP0000312397, MDP0000423544
Ethylene response factor (ERF)	ET/JA signaling	MDP0000235313, MDP0000127134, MDP0000880063
Endochitinase (PR-4) CHIB	Pathogenesis-related protein	MDP0000430546, MDP0000655939
MYC2	Transcription factors	MDP0000029168
WRKY33	Transcription factors	MDP0000708692, MDP0000935996
NahG	Pathogenesis-related protein	MDP0000188175
Chalcone synthase (CHS)	Phenylpropanoid biosynthesis pathway	MDP0000431621, MDP0000686666, MDP0000067565, MDP0000302905
Beta-glucosidase (Beta-gluc)	Phenylpropanoid biosynthesis pathway	MDP0000175949, MDP0000315857
Flavonol synthase/flavanone 3-hydroxylase	Phenylpropanoid biosynthesis pathway	MDP0000218810
Biphenyl synthase 3 (BIS3)	Phenolics biosynthesis	MDP0000287919
Biphenyl synthase 2 (BIS2)	Phenolics biosynthesis	MDP0000208899, MDP0000432621, MDP0000716308, MDP0000168735
Spermidine synthase (SPDS)	Secondary metabolisms	MDP0000198590, MDP0000294813
Cytochrome P450	Secondary metabolisms	MDP0000678795
2-Oxoglutarate/Fe (II)-dependent dioxygenase	Secondary metabolisms	MDP0000128879
NAD(P)-linked oxidoreductase	Secondary metabolisms	MDP0000857724
Omega 3-fatty acid desaturase	Secondary metabolisms	MDP0000127630, MDP0000156530
Mandelonitrile lyase	Hydrogen cyanide generation	MDP0000318256
Cyanogenic beta-glucosidase	Hydrogen cyanide generation	MDP0000047586, MDP0000805281
Squalene monooxygenase	Terpenoid biosynthesis	MDP0000168437
Cytokinin hydroxylase	Cytokinin biosynthesis	MDP0000305091, MDP0000747755

In other pathosystems, the activation of these genes is known to play a role in deterring pathogen progression and proliferation in plant tissues. The induced production of anti-microbial metabolites, such as those from the phenylpropanoid biosynthesis pathways, at the localized infection site is believed to be one of the major mechanisms implicated in disease resistance. The hypothesis to be tested in this study is that the differential expression patterns of these genes contribute to genotype-specific apple root resistance responses to *P. ultimum* infection. All these genes were subjected to multi-sequence alignment analysis and gene-specific primer design before characterizing their expression patterns using quantitative reverse transcription polymerase chain reaction (qRT-PCR) method.

3. Differential expression patterns for selected candidate genes among rootstock genotypes

The overall gene expression data identified several apple candidate genes with variable expression patterns between tolerant and susceptible apple rootstocks. There was an elevated expression level for most of the tested genes in susceptible cultivars B.9 and M.26 in the early stage of infection; however, the induced expression quickly faded away for most of the tested genes. In contrast, there were a few genes that exhibited sustained activation in the tolerant cultivars of G.41 and G.935.

Table 3. Heat map representation of the activation levels of apple candidate genes among rootstock cultivars during the infection processes.

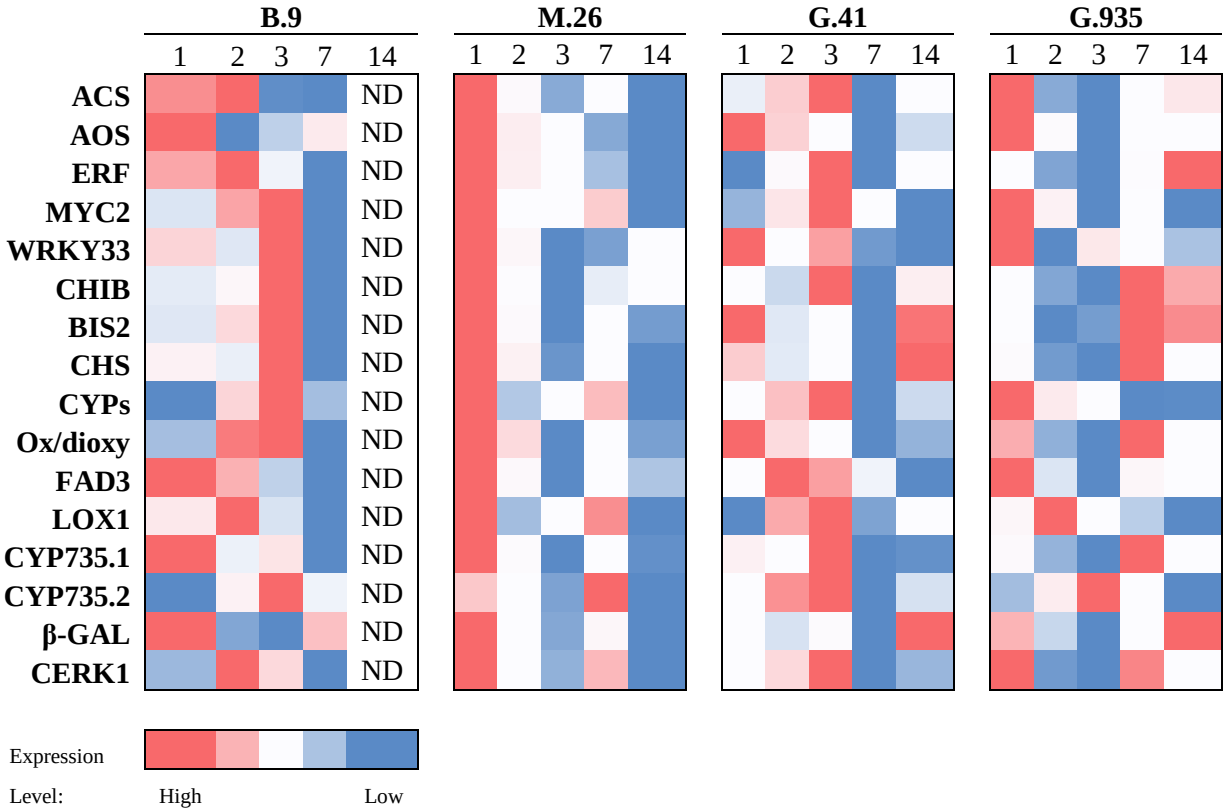

The level of induction was expressed as the relative fold change in infected tissues compared with the level in the mock inoculated tissues at the same time points. The darker red color represents the higher fold increase of gene activity in infected root tissue in relation to mock inoculation control; on the other hand, the darker blue color represents the lower fold change.

MdCHS (MDP0000431621), which catalyzes the early step of phenylpropanoid biosynthesis pathway, was highly induced in G.935 at 7 dpi, and a ß-endochitinase (or pathogenesis related protein 4) encoding gene

(*MdCHIB*: MDP0000430546) was induced at a higher level in the root tissue of G.935 and G.41, as compared to B.9 and M.26. In other pathosystems, it has been established that the key transcription factors of WRKY33 directly regulate the secondary metabolism in the process of generating antimicrobial metabolites. The gene expression patterns of *MdWRKY33* (MDP0000708692) showed different activation patterns between tolerant and susceptible cultivars. A gene encoding a ß-glucosidase (*MdGluc*: MDP0000175949), which is mapped to later phenylpropanoid biosynthesis pathway, exhibited a stronger induction toward the later stage in roots of tolerant cultivars G.41 and G.935, compared to those in B.9 and M.26. A gene encoding a homolog protein of chitin elicitor receptor kinase (or CERK), functions in detection of the pathogen presence and early activation of defense response. The CERK encoding gene (MDP0000136494) showed an earlier and stronger activation in the root of G.935, although it is also activated early in M.26. Therefore, it is possible that the activation of CERK is an essential part for the early stage of the defense activation; however, the coordinated activation of later-steps in secondary metabolism could also be critical.

Variation in the innate immunity responses for individual apple rootstock genotypes ultimately determines the outcome when challenged by ARD pathogens, in this case *P. ultimum*. The capability in early detection of pathogen presence, the strong activation of defense pathways and the production of antimicrobial metabolites are possibly the key to limit pathogen progression in the roots of G.935 and G.41. Similarly, the inability to foil "attacks" from pathogens, such as detoxification of damaging pathogen-derived chemicals, could also terminate effective defense response in B.9 and M.26. To our knowledge this is the first attempt to associate specific apple genes with a role in defending against attack by ARD pathogens. It will require additional experiments to exclusively and definitively identify the functional apple disease defense response genes including comparative transcriptome analysis using apple germplasm with well-defined resistance phenotypes.

4. Validating the selected genes using phenotyped accessions from O3 x R5 population

Figure 5A. A representing images showing variable resistance responses to infection by *P. ultimum* among O3 x R5 accessions

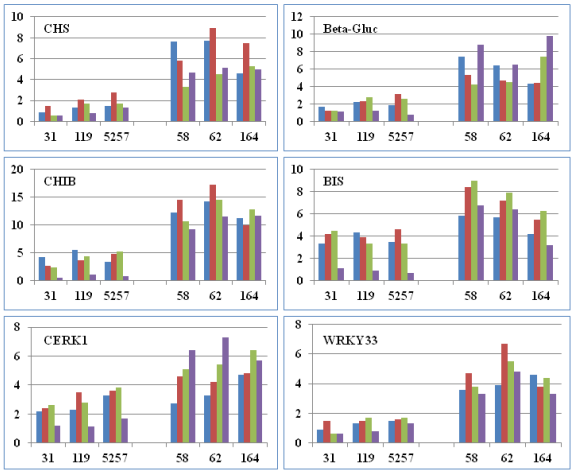

Figure 5B. Expression patterns for selected genes among O3 x R5 accessions

Figure 5. The expression patterns of six selected genes in response to *P. ultimum* infection between two groups (highly resistant and susceptible) of apple rootstock genotypes from O3 x R5 accessions. A: a representing image showing different resistance responses among individual accessions in O3 x R5 cross population. B: distinguishable gene expression patterns for selected six candidate genes between the more susceptible accessions (31, 119 and 5257) and the more resistant accessions (58, 62 and 164). Values on the Y axis are the fold changes after calibrating with the value from 0 dpi, i.e. the root sample before

inoculation assay, and normalized to the expression level in mock inoculated tissue at the same time point. The blue, red, green and purple bars (or from left to right) in each group of bars represent the time point of 1, 2, 3 and 7 dpi.

Six phenotyped accessions from O3 x R5 population showed more extreme resistance or susceptibility compared to the observed responses between B.9 and G.935. Among these accessions, no.58, 62 and 164 exhibited higher level of resistance as indicated by survival rates at the end of 30 days, while accession no.31, 119 and 5257 showed the extreme susceptible phenotypes such as earlier and more severe wilt symptoms. Four out of six tested genes, i.e. CHS, Beta-Gluc, CHIB and WRKY33, showed distinct expression profiles between two groups of rootstocks. These gene expression data for the selected candidate genes are in general aligned with those data using core collection of apple rootstocks, i.e. B.9 and M.26 versus G.41 and G.935.

5. Differential activation of selected candidate genes in response to infection by various ARD pathogens

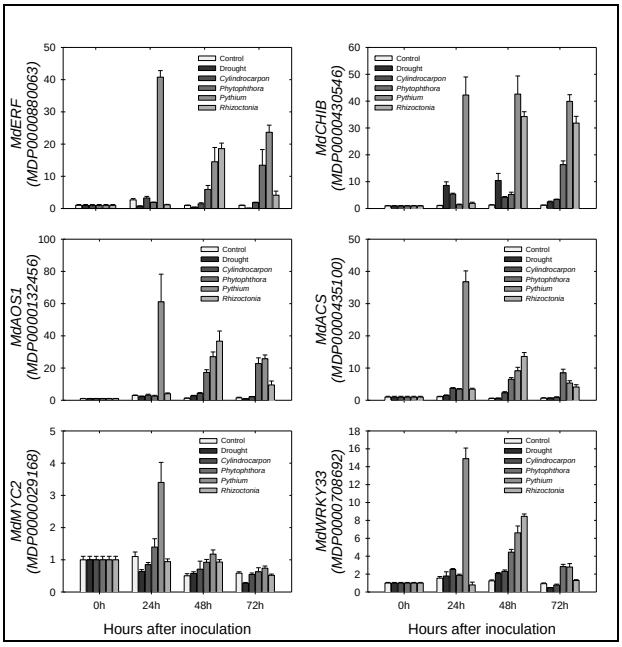

Most of the selected genes were known to be induced by *P. ultimum* infection based upon a previous study. However, their expression patterns as challenged by other ARD pathogens have not been examined. As shown in **Figure 6**, the preliminary data suggested that, at least to these selected genes, their activation seemed to be more responsive to infection by *P. ultimum*, compared to other ARD pathogens. In particular, the highest expression levels were observed at 24 hpi for these tested genes. As controls, mock inoculation or the drought treatment did not activate the expression of these genes.

Figure 6. The expression patterns of selected candidate apple genes in response to the infection to *P. ultimum* and other ARD pathogens as well as drought treatment. Plants used in this experiment were those from apple (cv Gala) seed germination. Each group of bars represents a time point as indicated on X axis. Within each group of bars, from left, were control, drought treatment, inoculated by *Cylindrocarbon*, *Phytophthora*, *Pythium ultimum* and *Rhizoctonia solani* AG5. The values of expression level at 0 hr, i.e. before inoculation, were arbitrarily set as 1 for comparison of various treatments.

EXECUTIVE SUMMARY

The differential responses of apple rootstock genotypes to infection by ARD pathogens have been observed from both field evaluations and greenhouse based investigations. Nevertheless, the genetics behind such variations are unknown. Accurate and reliable phenotyping of apple rootstock germplasm in response to ARD pathogen infection is a critical prerequisite to identifying the underlying genetic components. Therefore, establishing the detailed and quantified phenotyping protocol was an important part of this study. Due to the complex etiology of ARD, *P. ultimum* was selected as a representative ARD pathogen in the current study. Defined plant materials that were generated by tissue culture procedures were utilized to characterize the resistance responses under controlled environment conditions. Distinct resistance responses were observed between the susceptible B.9 and the tolerant G.935. The accessions in O3 x R5 population exhibited even more extreme susceptible or resistant phenotypes. Building on the observed resistance phenotypes, apple candidate genes were selected based on the results of a previous transcriptome analysis. Specifically, forty three (43) candidate apple genes were screened for their differential expression patterns between tolerant G.41 and G.935, and susceptible M.26 and B.9. More distinguishable expression patterns were observed for several candidate genes among the phenotyped accessions from O3 x R5 population. Our data indicated that the differential resistance responses at the biological, microscopic and gene expression levels may ultimately contribute to the contrasting survival rate between B.9 and G.935 as they were challenged by the same preparation of *P. ultimum*. This dataset provided a foundation for more definitive and conclusive association between specific apple genes and different levels of root resistance among apple rootstock germplasm. Our phenotyping work will expand to other members within the ARD pathogen complex, and extend to the evaluation under field conditions.

Plant-pathogen interactions can be described as a "chemical warfare" between two partners. The capability in timely and efficient production of antimicrobial compounds (phytoalexins), releasing preformed metabolites (phytoanticipins), or detoxifying the pathogen-originated toxin have been shown to contribute to disease resistance in other pathosystems (Ahuja et al., 2012; Chizzali et al., 2012; Grayer and Kokubun, 2001; VanEtten et al., 1994). The observed strong deterrence of the fast-growing *Pythium* in the root of G.935 may reflect the effective defense mechanism by efficient accumulation of antimicrobial metabolites. On the other hand, inadequate production of antimicrobial metabolites in the root of B.9 could have allowed rapid necrosis along the root of susceptible B.9. The observed variations of their survival rate could largely attribute to the difference in defense reaction. Applying other advanced approaches should further narrow down the candidate genes and/or metabolites which are responsible for the observed necrosis development in G.935. For example, the comparative transcriptome analysis between G.935 and B.9 should assist enormously in attempt to pinpoint the specific genes robustly associated with observed apple root resistance or susceptibility to *P. ultimum* infection. Identification of apple genes associated with resistance phenotypes will be the basis for developing molecular tools for efficient and accurate incorporation of the resistance traits into next generation apple rootstock. Maximized utilization of plant innate immunity will reduce, even eliminate, the need of chemical fumigants in managing ARD in the future, and improve the soil quality for sustainable production system. Therefore, results from current study are directly related to the sustainability of Washington State apple industry.